Experimental validation of a low-head turbine intake designed by CFD following Fisher and Franke guidelines

M Angulo[1], S Liscia[1], A Lopez[2] and C Lucino[1].

[1]Laboratory of Hydromechanics, University of La Plata, La Plata, Argentina
[2]Faculty of Engineering, University of Asunción, Paraguay

E-mail: mauricio.angulo@ing.unlp.edu.ar

Abstract. Model acceptance tests evaluate the response of the turbines at different operating conditions. Model tests are mounted so that the velocity profile at the inlet section is uniform, a condition which is not often met in practice. In fact, divergences might render inaccurate model results, obtaining at prototype scale an efficiency drop, structural vibrations and even component failures, in extreme cases. This concern becomes all the more relevant for low-head turbines, as the intake is closer to the turbine runner. With the aim of best estimating the actual flow conditions at the turbine inlet section as a function of the intake design, Voith designers, Fisher and Franke recommended performing scale model tests of the intake structure and listed a series of requirements that a good intake design should meet. These guidelines have not yet been applied on numerical modeling design but rather on more expensive and time-consuming scale model tests.
This work presents the results of a computational fluid dynamics (CFD) design of a low-head turbine intake taking into account an upgraded version of Fisher and Franke recommendations. The optimization process was aimed at obtaining the design that best matches the ideal flow conditions at the inlet section. The physical model was built in a scale of 1:40 and involves the complete turbine intake geometry. Different designs were tested on the basis of the evaluation of their corresponding velocity field distributions at a reference section and the best design was measured with an acoustic Doppler velocimeter (Vectrino). The results show that intake design guidelines are very useful tools that allow hydraulic designers to test their proposals with CFD more quickly, objectively and with enough degree of sensitivity to optimize the intake geometry.

1. Introduction

Turbine intake design has a relevant influence on the future performance of power units. The early detection of a poor intake design will prevent the decrease of energy production, increase the reliability turbine components - due to reduction of vibrations - and prevent component failure in extreme cases [1].

In order to deal with this problem Fisher and Franke - Voith designers – have given a set of guidelines for a good intake design as a conclusion of three turbine manufacturers and their own experiences. These guidelines have been applied to physical model tests to conduct studies in order to improve flow characteristics at low head turbine intakes. Recently these guidelines have been upgraded and have been applied to a numerical modeling optimization of low head turbines [2].
Another relevant fact is that when a turbine acceptance test is performed, it is done with the working hypothesis that flow at the turbine inlet has a flow pattern without distortions, that is, ideal conditions. Such ideal conditions are hardly ever reached in real power stations. Therefore, the aim of these guidelines is to help turbine designers to improve their intake geometries.

Main doubts about CFD results, especially when an optimization process is carried out, are if they are reliable or not, and if it possible to trust only in them without testing physical models, as it has been traditionally done in hydraulic engineering over the last decades. For this reason, the main objective of this work is to validate, by means of a physical model test, the results of an optimized design modeled with a CFD code. A secondary objective is to prove how useful the application of the optimization process is when following the upgraded guidelines of Fisher and Franke designers, and testing the best design on a physical model.

The particular case study belongs to a power station that will be built on an existing spillway structure. The existing project has two spillways and a power station with a 3200 MW of installed capacity. The power station and one of the spillways return water to the main branch of the river, the other spillway returns water to a secondary branch. The future power station has two objectives: the first is to allow flood passage over its structure without compromising the safety of the whole project; and the second is to take advantage of the flow released for ecological reasons. A cross section of the project and the optimized design are shown in Figure 1.

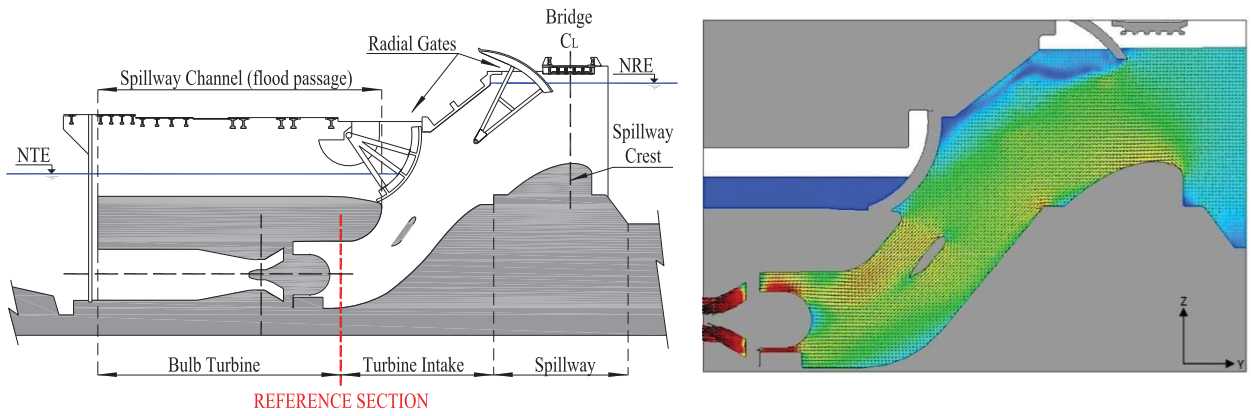

Figure 1. Left: Cross section of the project. Right: CFD-optimized design of a bulb intake

This work is ongoing in the context of the counseling work that the National Universities of La Plata (UNLP) and Misiones (UNaM) carry out for the Binational Entity of Yacyretá (EBY) of the Argentina and Paraguay Republics. The Laboratory of Hydromechanics from the Faculty of engineering (UNLP) and the Center of studies for Energy and Development (CEED) are the executing units of the expansion project of the Yacyretá Hydropower complex.

2. Methods and Materials

2.1. Numerical simulation

2.1.1. CFD code Features. The CFD modeling was done by means of FLOW-3D code. This software is a general-purpose code and solves the Navier-Stokes equations by the method of finite volumes/finite differences in a structured rectangular grid. Flow-3D uses a Fractional Area/Volume Obstacle Representation Method to represent the solid obstacle from which all the equations used are reformulated as functions of the area and volume porosity. This method, called *FAVOR* method, allows the modeling of complex geometries.

An advantage of using this code compared with others is that grid building is independent of the geometry. Therefore, it is suitable for optimization processes where changes in geometry are made in each new simulation, saving time on meshing task. This feature is also an advantage when more refinement is required to reach a more detailed solution. It is also possible to use several block meshes, linked or nested, to represent different scale phenomena.

2.2.2. Numerical model set-up. The modeled geometry represented only one unit and not the complete power station. Since flow has three dimensional characteristics, a 3D approach was used. Reynolds-Averaged Navier-Stakes equations (RANS) were employed to solve simulations. The turbulence model chosen was the k-ε RNG. A constant mixed length of 1,19m was set, calculated as the 7% of the fluid depth at the spillway crest.

The domain was discretized by three orthogonal meshes: one mesh containing the inlet channel (representing the reservoir); a central mesh which involves the spillway, the turbine intake and part of the internal geometry of the bulb turbine up to the runner section; and a mesh at the draft tube (see Figure 2 and Table 1). It is important to clarify that it is not the intention of this work to model the turbine internal flow, but the turbine intake. As changes in geometry were very near to the turbine inlet, a reference section was defined a few meters upstream the bulb, so the turbine geometry impacted on the flow velocity profile. This is the reason to model part of the internal geometry.

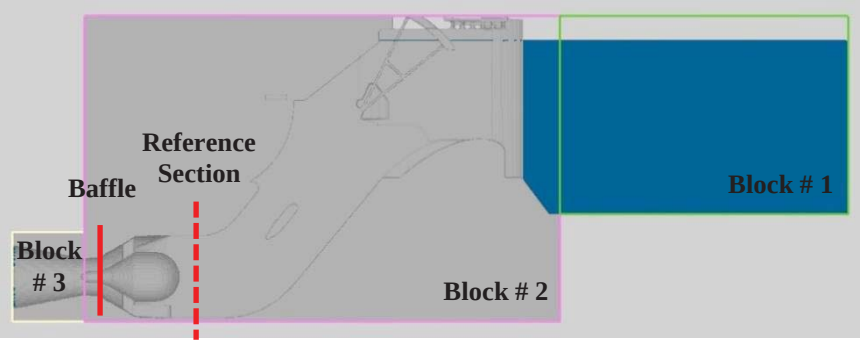

Figure 2. Domain discretization

The absolute roughness of geometry components was set on 1 mm to represent concrete roughness.

The boundary conditions are specified pressure/fluid height upstream the mesh 1 and downstream the mesh number 3. For the rest of the boundaries, symmetry condition was set. The fluid height represented upstream corresponded to the normal reservoir elevation (NRE) and downstream the fluid height is a normal tailwater elevation. This difference of total energy between the domain inlet and outlet established a permanent flow through the turbine. In order to achieve the nominal flow of this bulb turbine, a baffle was placed at the turbine runner centerline with porosity properties to produce a local head loss. After some iteration, a quadratic loss coefficient equal to 1.75, which fulfilled this condition, was found. The linear loss coefficient was set on zero.

The simulation was divided into two stages. The 1st stage consisted of running with a coarse mesh for 200 seconds until steady flow conditions were achieved. The final results of CFD calculation are extracted from the 2nd stage simulation with fine mesh and 100 sec length, until flow was stabilized. In table 1, more details about meshes on each stage are shown.

Table 1. Mesh features

Mesh Block	1st Stage		2nd Stage	
	Size (m)	Cells #	Size (m)	Cells #
1 (Reservoir)	0,50	241.000	0,50	241.000
2 (Turbine Intake)	0,50	612.000	0,25	4.450.000
3 (Draft Tube)	0,50	27.000	0,50	27.000
Cells #	Total	880.000	Total	4.718.000
	Active	489.000	Active	1.850.000
Simulation time (sec)	200		100	

2.2. Physical model test

2.2.1. *Experimental set-up.* The physical model test was built with solid materials (acrylic, plastics and stainless steel) in a 1:40 scale. The model reproduced one turbine vane identically as it was modeled with CFD code. Taking into account the proximity of the reference section to the bulb inlet, the scale model represented part of the bulb geometry such as the bulb itself, the pedestal and the transition section from the inlet to the wicket gate. At the runner section an orifice plate was installed in order to obtain the turbine flow rate.

The boundary conditions are constant flow and level at the intake, representing the nominal flow of the bulb turbine and the normal reservoir level. The model was installed in a closed circuit, downstream a constant level chamber, which guarantees that flow at the inlet and has no fluctuation coming from the circulating pump. Downstream level was controlled by an adjustable bottom gate in order to obtain the upstream level at the intake. The upstream level is the normal reservoir elevation. Flow was controlled by a sluice valve and measured by a standardized nozzle installed in the circuit, having an accuracy of +/- 1%. Upstream level was measured by a limnimeter with a precision of +/- 0.5mm. As the inlet channel has a non-negligible velocity, kinetic energy has been taken into account to correct the total energy level upstream the spillway inlet. Both the test section and the physical model set-up are shown in Figure 3.

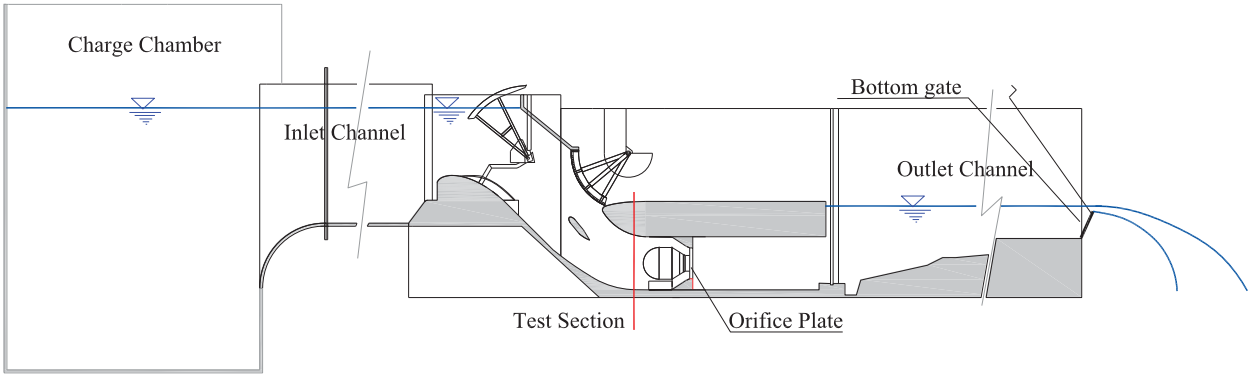

Figure 3. Physical model scheme

2.2.2. *Measuring equipment and data processing.* In order to survey the velocity profiles at the reference section, an acoustic Vectrino velocimeter (lab probe, as it is commercially named by Nortek) was used

and it was mounted on an especial device. The device was built in order to measure at a pressurized section and had 5 holes, one for each survey profile. It also had a screw to tight the vertical position of the velocimeter (See Figure 4).
The cross section has a dimension of 331,2mm height and 356,2mm wide. Velocity was measured across five profiles on seven points for each one, being a total of 35 points surveyed. When a new profile was measured, the circulating pump was turned off and the model bay emptied in order to change the Vectrino position. Each point was measured for 7 minutes at a sampling rate of 50 Hz. The data logged has the three components of velocity. The accuracy of the instrument is +/- 0.5 % of the measured value as it is indicated by the manufacturer.

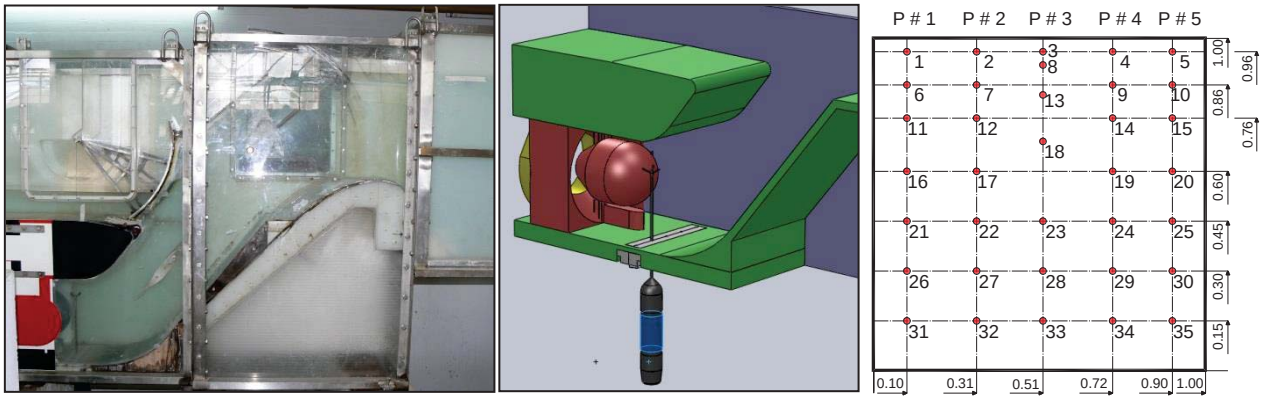

Figure 4. Left: Physical model picture. Center: Test section especial device. Right: Measurement grid

2.3. Data processing

For both CFD and experimental results, the flow field at the reference section was extracted. The upgraded F&F requirements were checked in order to compare results. A quick review of the flow requirements and the way to check them in mentioned in the subsequent paragraphs.

Req. # 1: The normalized axial flow velocity (Vyn) at the reference section should be as close as possible to the spatial distribution named "Ideal" flow condition.
The normalized axial flow velocity must be calculated as follows: *Vyn [-] = Vy/Uy*, *Uy* is the mean axial velocity. *Vyn* values must be in descending order. Then, to curves can be plotted: one for *Vyn* > 1 and the other for *Vyn* < 1. The abscissa indicates the accumulated area that equalizes or exceeds a particular value of *Vyn*. (Figure 8 – upper left image)

Req. # 2: At reference cross section, no cross flow velocity should exceed +/- 5 % of mean axial velocity (Uy).
A~~n~~ histogram for each of the normalized velocities *Vxn* (horizontal direction) and *Vzn* (vertical direction) must be calculated as follows:

$$V_{xn}[\%] = \left|\frac{V_x * 100}{U_y}\right| \qquad V_{zn}[\%] = \left|\frac{V_z * 100}{U_y}\right|$$

The histogram contains the normalized velocity value (*Vxn* or *Vzn*) in abscissas and the relative frequency in the ordinate. (Figure 8 – lower right image).

Req. # 3: Flow free from air-entraining vortices.
Req. # 4: Deviation of flow for each quadrant should not vary more than 10 %.
The reference section was divided in four quadrants in order to compute flow: Q_1, Q_2, Q_3, Q_4. .Then the flow deviations were calculated as follows:

$$dQ_q\,[\%] = \left(\frac{Q_q}{Q_t}\right) * \left(\frac{A_q}{A_t}\right)$$

The subscript "*q*" indicates the quadrant order. "*Qt*" is the total flow and "*At*" is the total area of the reference section. The results were plotted on a graph with the quadrant order on abscissas and the flow deviation on the vertical axis. The quadrants 1 and 2 are upper ones and the 3 and 4 the lower ones. (Figure 8 – upper right image).

Req. # 5: The deviation angle of flow velocity from axial direction should not exceed 5º. This value could be exceeded only if it did not result in a rotating flow.
To evaluate this requirement the histograms of deviation angles α (XY plane) and β (ZY plane) were computed.

$$\alpha[^\circ] = arc\tan\left|\frac{V_x}{V_y}\right| \qquad \beta[^\circ] = arc\tan\left|\frac{V_z}{V_y}\right|$$

The histograms show the α angle on abscissas and the relative frequency on the ordinate. The same was done for β angle (Figure 8 – lower left image).

Req. # 6: The α Coriolis coefficient at the reference section should not exceed 5 % from the value calculated for the "Ideal" flow condition.
The correction factor for the kinetic energy named α Coriolis, was computed for the reference section by means of the following expression:

$$\alpha_c[-] = \frac{\sum\left[\left(\frac{V_{yi}}{U_y}\right)^3 * A_i\right]}{\sum A_i}$$

The subscript "i" corresponds to the cell order. When computing CFD results calculated with FLOW-3D® code, as it is our case, it is necessary to consider the Fraction of Fluid (FF) and the Volume Fraction (VF) of each cell in order to know the actual fraction of the cells filled with fluid. This area must be computed with this expression: $A_i = A_{cell}$. FF . VF

Since the axial flow velocity (Vy) distribution is the most affected component due to turbine intake geometry changes, it was used to compare CFD and Experimental results. For both, axial velocity was normalized by the mean axial velocity (Uy). Physical model results were first scaled to prototype. 2D velocity profiles were computed with Surfer software. In the case of CFD data, the grid density is the same as computational grid (0,25 m). For the physical model velocity profile, a velocity of cero it was added on the wall and the grid was made denser than the measurement grid. A kriging interpolation method was used in order to obtain values in a grid with the same density as the prototype (0,25 m), (Figure 5).

1D velocity profiles were plotted for CFD and Experimental data. In this case, only the measured point it was plotted with its corresponding error bar of +/- the standard deviation. The depth is shown in a normalized scale to simplify its interpretation (Figure 7).

3. Results

3.1. Numerical and Experimental Results

As it was mentioned before, 2D normalized velocity profiles for the reference section were calculated and plotted on Figure 5. Also the modulus of the relative error between CFD and experimental was calculated and plotted on Figure 6.

A comparison between each of the five profiles surveyed was made (Figure 7). The CFD results are indicated with a red continuous line and the experimental data was joined with a blue dash line.

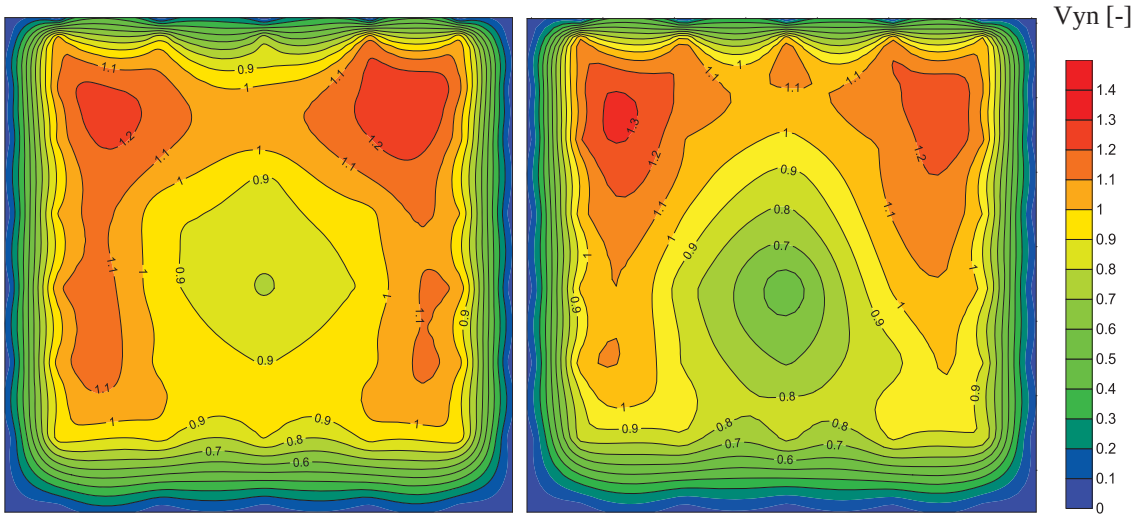

Figure 5. Left: CFD velocity field. Right: Experimental velocity field

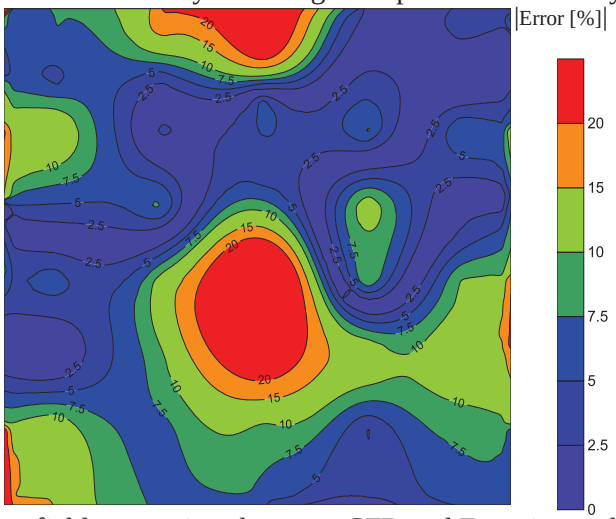

Figure 6. Flow field comparison between CFD and Experimental results

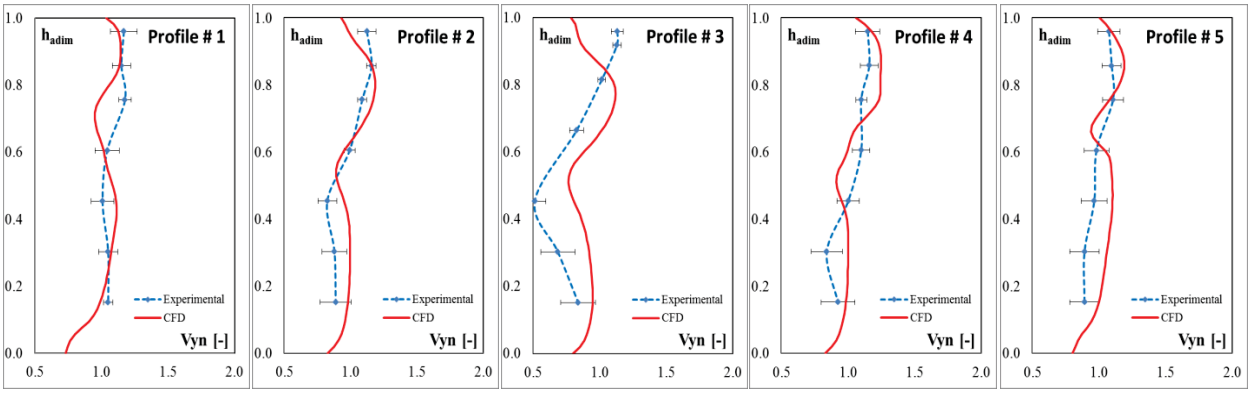

Figure 7. 1D Velocity profiles comparison between CFD and Experimental results.

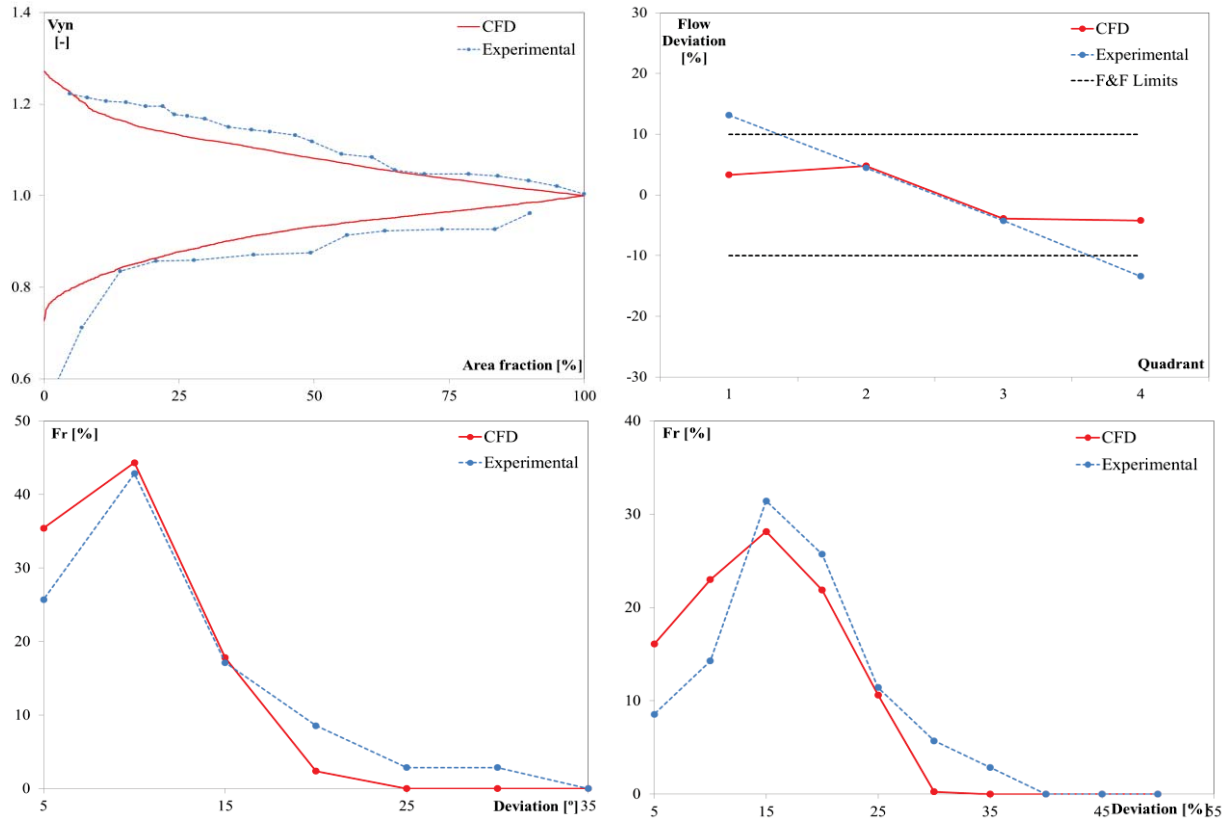

Figure 8. Comparison between CFD and experimental results of upgraded Fisher and Franke requirements. Upper left: Requirement # 1. Upper right: Requirement # 4. Lower left: Requirement # 5. Lower right: Requirement # 2.

The F&F guidelines were calculated for the requirement numbers 1, 2, 4 and 5. A red continuous line represents CFD results and a blue dash line represents physical model results.

The requirement number 3, which recommends free entraining vortices at the intake, was confirmed for physical model test as no vortices were detected at the intake.
The correction factor of kinetic energy, α Coriolis, was calculated for CFD and Experimental results. A value of 1,08 and 1,07, respectively, was obtained.

4. Discussion

In order to validate the CFD results with the physical model tests, we proposed to compare results for 2D and 1D velocity profile at the reference section and to evaluate the F&F recommendations for both.

The 2D velocity profile comparison was made using the normalized axial velocity (Vyn) in order to eliminate possible absolute differences between CFD and PM measurements. In Figure 5, we can see the same flow field pattern in both cases. Flow concentration on the upper quadrants and the stagnation point at the center of the section corresponding to the turbine bulb can be observed. Although this is a qualitative aspect, it is an important point because it means that CFD calculation hypotheses were right and allowed capturing the flow field.

From the quantitative point of view, in figure 6 the modulus of the difference between CFD and experimental data is shown. As it can be seen, most of the area is under 7,5 % of error which we consider acceptable. A central area with a high error (more than 20 %) also exists, probably due to the interaction of the turbine bulb with the Vectrino probe when measuring the physical model. This difference could be saved if a more distant section is chosen to survey.

The 1D velocity profiles give also an idea of the quality of the obtained results (Figure 7). 19 of the 35 cells of CFD results are under +/- one standard deviation from the corresponding surveyed points on the physical model test. The worst profile fitting is observed for the central profile (P # 3) - probably for the same reason mentioned in the previous paragraph - related to the proximity between reference section and measurements section.

The analysis of the upgraded F&F guidelines shows other features of the flow field distribution.
The requirement # 1 (Figure 8), shows a good agreement between CFD and PM for $1.2 < Vyn < 0.8$. For values outside this range the PM tends to give higher extreme values of Vyn up to 0.5 (corresponding to point # 23 near the center). This could be also consequence of the low density of the measurement grid.
The requirement # 4, which evaluates the flow distribution between quadrants, shows a good agreement for quadrants 2 and 3, but not for quadrants 1 and 4, where it can be seen a deviation slightly over of the maximum recommended of 10 % of deviation.

The requirement # 2 and # 5 expresses the deviation in magnitude and direction of the cross flow (in this case Vx). In both cases the frequency histograms shows good agreement compatibility with experimental data (Figure 8 – lower graphs). The deviation angle differences of relative frequency are less than 5 % for most of the curve, except for 5º of deviation where the PM indicates that the amount of vectors with this deviation is lower. For the magnitude deviation, it is observed that in PM test the cross flow has a slight difference over the CFD results of about 5 % for deviation greater than 15%.

For the last requirement, the # 6, the Coriolis coefficients are very near, with a difference of 0,01. This is an interesting result taking into account that this parameter in sensitive enough to detect changes in geometry [1].

It is important to observe that the analysis of the mentioned requirement was done with a number of 3132 grid points extracted from CFD results, and for the experimental results, only with 35 points. Even though results do not present big differences, they let us conclude that a denser measurement grid will improve substantially the compatibility between CFD and PM. This could be done by means of a more powerful measurement technique such as Particle Image Velocimetry (PIV).

5. Summary and Conclusions

This work showed the validation of CFD results with experimental measurements. The CFD results come from the optimization process for a low head turbine intake, where this process was guided with the upgraded F&F recommendations. The best and final design of this intake was reproduced on a physical model scale of 1:40 and was tested for the nominal turbine flow. The velocity field at the reference section was surveyed with an acoustic Doppler velocimetry technique.

Both CFD and PM data were processed and analyzed. As a result, 1D and 2D velocity profiles were extracted. Besides this, the F&F requirements were processed in order to characterize the flow field at the reference section.

The CFD simulation showed good compatibility with experimental measurements. One of the most important facts is that the simulation can capture the pattern of flow at the inlet section because this is the key for reliable results of optimization process based only on the velocity field distribution. This could be demonstrated by comparing normalized velocity fields and profiles from both approaches.

It has also been proved that the upgraded design guidelines are simple but powerful tools to guide a design process as almost the same results can be obtained working with physical model data or CFD calculations. We should not forget that originally these criteria were used only on a physical model test which provides less information than CFD calculations, and takes more time and money.

As a conclusion, the present work based on experimental data encourages turbine designers to use numerical tools to model turbine intakes, especially for low head turbines where the intake design affects the internal flow of the machine. It also attempts to give support along the optimization process following the upgraded F&F guidelines in order to get a more objective comparative analysis of alternatives.

Acknowledgements

We would like to thank EBY (Entidad Binacional Yacyretá) for the support and finance of this work.
This study is made possible through the help of Yacyretá entity (EBY), which gives us financial support to carry out the model experiment. We also appreciate the work of Juan Agustín Parravicini, member of our Laboratory, in the physical model measurement tasks.

References

[1] Fisher F K Jr, and Franke G F, 1987: The Impact of Inlet Flow Characteristics on Low Head Hydro Projects. International conference on hydropower , Porland, Oregon.
[2] Angulo M, Liscia S O, 2013: CFD optimization of low head turbines intake design using Fisher-Franke guidelines. I IAHR Latin American Hydro Power ans Systems Meeting, Campinas Brasil.
[3] Lichtneger P, 2009: Intake Flow Problems at Low-Head Hydropower. Wasserbaukolloquium: Wasserkraft im Zeichendes Klimawandels Dresdener Wasserbauliche Mitteilungen Heft 39
[4] Zhao Y P, Liao W L, Feng H D, Ruan H and Luo X Q, 2012: Experimental and numerical study on inlet and outlet conditions of a bulb turbine with considering free surface. 26th IAHR Symposium on Hydraulic Machinery and Systems. Beijing, China.
[5] Fošumpaur P, Čihák F, 2005: Design and Optimization of a Turbine Intake Structure. Czech Technical University in Prague, Acta Polytechnica Vol. 45 No. 3
[6] U.S. Bureau of Reclamation Engineering and Research Center. Hydraulic Model Studies on Bulb Turbine lntakes; REC-ERC-82-14, March 1983